Iterative Design Process of a Robotic Compliant Gripper for Kiwifruit Harvesting Using Topology Optimization

Hung Phan Le*, Ben McGuinness, Christoff Venter, Eva Prinz, Mike Duke, Shen Hin Lim and Ajit Pal Singh**
School of Engineering, University of Waikato, Hamilton, New Zealand
hl379@students.waikato.ac.nz*, ajitpal.singh@waikato.ac.nz**

Abstract

Compliant mechanisms offer distinct advantages for agricultural robotics by reducing weight, eliminating joints, and simplifying fabrication. This study presents a parameter-driven, iterative design approach for developing a two-finger compliant gripper for kiwifruit harvesting, utilising two-dimensional topology optimization in Altair OptiStruct (HyperWorks). Key design parameters including geometry, boundary conditions, compliance constraints, material volume fractions, and density thresholds, were systematically varied and evaluated using finite element analysis (FEA), rapid prototyping, and Digital Image Correlation (DIC) experiments for validation. Early iterations focused on displacement and stress behaviour, while later designs incorporated gripping force requirements identified from harvesting studies. The final prototype (G8) satisfied displacement, stiffness, and structural performance under load criteria, overcoming the limitations observed in earlier designs (G1–G7). These conclusions are based on simulation results, with experimental validation currently in progress. Overall, the work delivers the first parameter-performance map for compliant grippers in kiwifruit harvesting and offers practical design guidelines for future agricultural robotics, including alternative materials, advanced additive manufacturing, and field-based testing.

1 Introduction

The kiwifruit industry in New Zealand plays a vital role in the national economy, generating billions in export revenue annually. However, the industry depends heavily on seasonal labour, making it highly vulnerable to workforce shortages, rising labour costs, and fluctuations in availability due to factors such as border closures, weather disruptions, and competing horticultural demands [Saeed, 2021]. During peak harvesting periods, growers face increasing difficulty securing enough skilled workers to pick fruit at the optimal ripeness window, leading to unharvested crops, financial losses, and reduced market competitiveness. Labour costs now account for a significant fraction of overall production expenses, placing mounting pressure on growers to find reliable, long-term solutions

The development of robotic harvesting systems has therefore become a strategic priority for the industry, promising to stabilise production costs, mitigate labour shortages, and ensure timely harvesting critical [Rajendran *et al.*, 2024; Xiao *et al.*, 2024]. Yet, unlike controlled industrial environments, orchard conditions are highly variable: fruit size, orientation, and foliage density change across trees and seasons, requiring harvesting robots to handle delicate fruit efficiently without causing bruising or damage. For these reasons, end-effectors or grippers have emerged as one of the most critical components in any robotic harvesting system, as they directly interact with the fruit and largely determine picking success.

Conventional rigid grippers, typically designed using multiple mechanical joints and linkages, present several limitations in orchard environments. Their large mass and size reduce dexterity, backlash between mechanical parts affects precision, and frequent maintenance needs limit long-term reliability [Xie *et al.*, 2022]. Moreover, rigid designs struggle to adapt passively to fruit variability, often requiring complex sensing and control systems to prevent damage during picking. Compliant mechanisms provide a promising alternative. By transferring force and motion through elastic deformation rather than discrete joints, they enable single-piece, joint-free structures that are lighter, simpler to fabricate, and inherently better at distributing contact forces. Their structural flexibility reduces assembly complexity, lowers friction and wear, improves reliability, and enhances motion precision, making them well-suited for orchard automation and other agricultural applications [Howell, 2001].

Several approaches exist for designing compliant mechanisms, including the pseudo-rigid-body method, analytical synthesis, and numerical optimization techniques [Gallego and Herder, 2009]. Among these, topology optimization has gained significant attention because it can automatically distribute material within a design domain to produce lightweight, joint-free structures without requiring predefined geometries. In gripper design, topology optimization enables compliant fingers to be directly generated from the design space rather than assembled from multiple rigid parts. However, its application to agricultural grippers remains challenging because performance requirements such as displacement, gripping force, and finger geometry are often undefined early in the design process. Existing designs typically rely on iterative adjustments and trial-and-error refinements rather than a structured workflow that quantitatively links parameter choices to functional outcomes.

Moreover, while topology optimization has been explored in soft robotic grippers, most studies target generic pick-and-place tasks under controlled conditions rather than crop-specific harvesting. Orchard environments demand additional considerations, including fruit accessibility within dense canopies, reliable gripping forces for variable fruit sizes, and minimal fruit damage under uncertain field conditions. This study addresses these gaps by presenting a structured, parameter-driven design framework for a compliant two-finger gripper tailored to kiwifruit harvesting. Rather than proposing a new optimization algorithm, it systematically links topology optimization parameters to displacement, stress, and gripping force outcomes, providing practical design guidelines for future agricultural robotics applications.

2 Background and Related Work

Several robotic systems have been developed for kiwifruit harvesting [Zhiwei *et al.*, 2025]. These systems typically include robotic arms to reach the fruit, vision systems to locate target fruit, and end-effectors to detach the fruit gently. For instance, Williams *et al.* [2019] introduced a kiwifruit harvesting system with four robotic arms, and built on this platform. Ting [2018] evaluated three different gripper shapes and found that certain design features resulted in less fruit damage compared to the other designs. Mu *et al.* [2020] designed another robotic system that applied two bionic fingers to grab fruit. Fu *et al.* [2024] proposed a multi-fruit envelope-cutting robot for kiwifruit harvesting. However, this latter approach does not meet New Zealand's postharvest requirements, which demand complete stem removal to avoid damaging adjacent fruits during storage and transport.

These limitations highlight a critical design gap: none of the existing kiwifruit harvesting systems explore the use of compliant grippers, despite their potential to combine gentle handling with mechanical simplicity. In contrast, research on other fruit-harvesting and pick-and-place applications has begun to adopt compliant mechanisms. For example, Miao and Zheng [2020] presented a compliant constant-force mechanism for apple harvesting. Xie *et al.* [2022] developed a bionic compliant end-effector for cherry tomato harvesting, inspired by the tarsal chain of Serica orientalis Motschulsky. Zolfagharian *et al.* [2022] introduced a bioinspired compliant soft gripper based on a spiral spring, demonstrating its effectiveness in handling fruits without causing damage.

Among the methods for designing compliant mechanisms, topology optimization has become a widely adopted strategy, particularly for grippers in soft object handling tasks. Liu *et al.* [2018] constructed a motor-driven compliant gripper optimized for grasping unknown objects ranging from 42 to 141 mm in size, with a maximum payload of 2.1 kg. Wang *et al.* [2020] applied topology optimization to a cable-driven soft robotic gripper for general pick-and-place tasks. Sun *et al.* [2022] introduced a 3D topology optimization-based adaptive gripper with a weight of only 180 g and a payload of 8.8 kg. Budzyń *et al.* [2023] proposed a compliant gripper designed to overcome the problem of lunar dust interfering with conventional jointed mechanisms. Liu *et al.* [2024] also designed a multi-material compliant finger for parallel grippers using topology optimization, showing adaptability to various object shapes.

Although these previous studies have demonstrated the potential of compliant grippers and the effectiveness of topology optimization in handling soft or irregular objects, their applications have been confined to conventional pick-and-place tasks or other fruit types with different harvesting requirements. Kiwifruit harvesting presents specific challenges, including the need to balance displacement, gripping force, and finger geometry while ensuring complete stem removal to meet New Zealand standards. These requirements are not clearly defined from the outset and cannot be addressed simply by adapting existing designs. This highlights the critical need to explore iterative design processes for compliant grippers, specifically for kiwifruit harvesting.

3 Methods and Materials

3.1 Topology Optimization

The compliant gripper was designed using two-dimensional topology optimization in Altair OptiStruct (HyperWorks). The approach followed the method proposed by Budzyń [2024]. The gripper was synthesized under two loading cases and was modelled as displacement-driven. To simplify the analysis, only the first load case, aligned with the intended motion, will be considered and presented in this study. A minimum member size filter of 3 was applied to avoid creating thin or non-manufacturable features. Since the gripper has two identical fingers, only half of the design space was modelled to reduce computation time (Figure 1). The resulting compliant mechanism works as follows: in its neutral position, the gripper is semi-open. When the input port moves downward, the fingers close, and when it moves upward, they open. This motion allows grasping a kiwifruit of different sizes. The design was intended to work with external soft sleeves for fruit protection, although sleeve development is outside the scope of this study. Nylon White (nylon 6) filament was selected as the material for fused filament fabrication.

3.2 Parameter Selection in Topology Optimization

Several parameters were varied to refine the optimized structures based on existing literature. These included:

- Design space (DS): Six design spaces were tested, representing simplified versions of a single finger. Some were inspired by existing rigid gripper layouts [Ting, 2018; Williams *et al.*, 2019], while others were modified geometries. In total, eight designs were generated.
- Boundary conditions: Input/output ports and fixed supports were adjusted to study how constraints and loads influenced structural behaviour.
- Compliance constraint (CC): Target values were tuned to balance output displacement and overall stiffness.
- Volume fraction (VF): Different material ratios were tested to explore density distribution and geometric complexity.
- Density threshold (DT): Applied in post-processing to eliminate intermediate densities and yield clear manufacturable shapes.

3.3 Finite Element Analysis

The 2D topology optimization results were refined in SolidWorks by increasing the gripper thickness to 10 mm. The gripper models were then imported into Ansys Workbench for FEA. Each model was evaluated in terms of displacement, stress distribution, and gripping force. The simulation process was carried out in two stages: (i) an early phase focused on displacement and stress distribution, and (ii) a later phase where gripping force was added once it was identified as a critical requirement for secure fruit handling. These analyses were used to evaluate whether the gripper achieved the desired displacement, whether the stresses had not exceeded the material yield strength, and whether the gripping force was sufficient for harvesting tasks while still preserving the desired motion of the compliant structure.

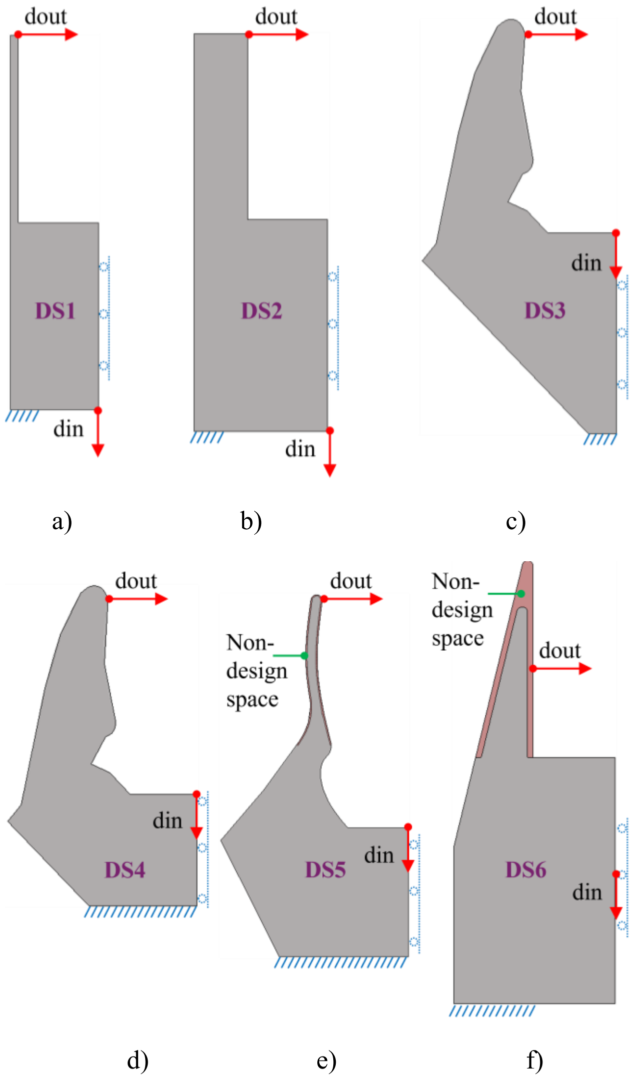

Figure 1: Design space configurations and boundary conditions for six gripper models. The shaded regions define the design spaces (DS1–DS6), with *din* and *dout* indicating the applied input and output displacements, respectively. Fixed boundaries are shown at the base, while non-design spaces are marked where applicable. (a) DS1, (b) DS2, (c) DS3, (d) DS4, (e) DS5, (f) DS6.

3.4 Prototyping and Functional Testing

Based on the results of topology optimization and FEA, eight gripper prototypes were fabricated using in-house 3D printing on a Markforged Mark Two printer with 100% infill to ensure structural integrity. After fabrication, all grippers were conditioned at room temperature to eliminate residual thermal effects before testing. Their functional performance was first evaluated under controlled laboratory conditions to characterise displacement and gripping behaviour. To investigate the influence of long-term moisture exposure on structural performance, one representative prototype (G6) was selected for additional experimental validation. This gripper was tested using DIC, which provided full-field displacement measurements for direct comparison with FEA predictions.

3.5 Structured Iterative Design Workflow

The design process followed an iterative workflow, captured schematically in Figure 2. It began with topology optimization in Altair OptiStruct (HyperWorks), where the DS, boundary conditions, and optimization parameters (CC, VF, DT) were specified. The initial screening involved a visual inspection to identify and eliminate designs with disconnected features, overly thin members, or excessively dense regions that produced unrealistic stiffness. For any discarded design, parameter refinements were introduced, and the optimization cycle was re-run until feasible outcomes were obtained. Throughout this stage, design feasibility and performance criteria guided the selection of promising configurations.

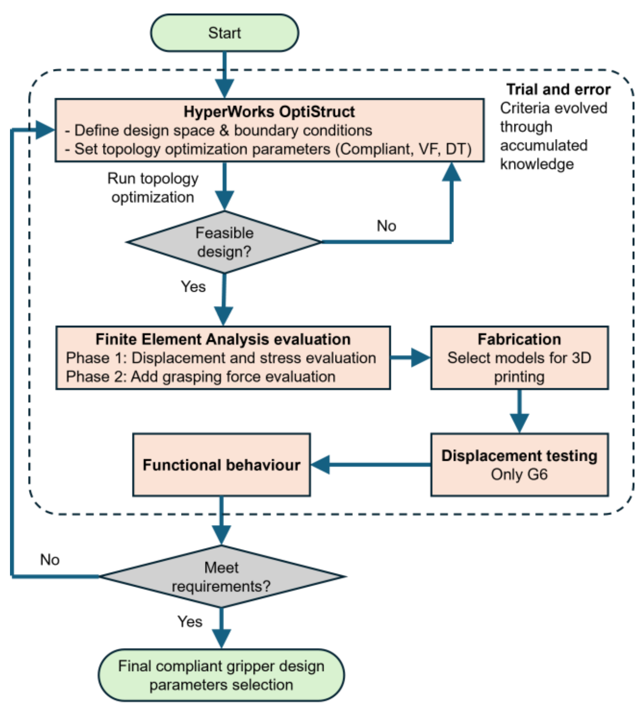

Figure 2: Structured Iterative Design Workflow.

Feasible topologies were then converted into 3D models with a uniform thickness of 10 mm and subjected to FEA. Based on these analyses, selected designs advanced to 3D printing using in-house fabrication facilities. Prototype-level testing involved closing-opening cycles and gripping motions under laboratory conditions, complemented by visual inspection to ensure compliance with harvesting requirements. Any prototype failing to meet motion or gripping criteria triggered a return to the optimization stage for further parameter adjustment, ensuring progressive refinement of the designs. When all performance metrics were satisfied, the final design parameters were established.

Building on this iterative workflow, diverse parameter combinations were systematically explored to generate multiple gripper models, each incorporating unique DS, CC, VF, and DT settings. These configurations were screened using FEA before physical prototyping, and the complete set of parameters with corresponding model identifiers is compiled in Table 1.

Table 1: Summarises the representative design spaces generated during the iterative design process. *G* represents the Gripper model. CC unit is N·mm.

Model	DS	CC	VF	DT	Description
G1	DS1	30	0.4	0.3	Thin fingers.
G2	DS2	30	0.4	0.7	Wider finger.
G3	DS2	15	0.2	0.5	Lower VF.
G4	DS2	15	0.2	0.5	Upward input.
G5	DS3	15	0.2	0.5	Rigid gripper M4 DS [Williams *et al.*, 2019].
G6	DS4	10	0.2	0.5	Shorter than DS5.
G7	DS5	8	0.2	0.6	Curve finger with non-design space.
G8	DS6	15	0.2	0.8	Output point at the middle of finger, M5 finger shape [Williams *et al.*, 2019]

4 Results and Discussion

4.1 Parameter Effects in Early Designs (G1–G4)

The first design iteration, G1, used a narrow finger (3 mm) with the output at the fingertip and the input at the bottom corner (Figure 1a). The design was too fragile, and the high compliance constraint (CC = 30 N·mm) required large input forces for relatively small displacements (Figure 3a). This highlighted the combined effect of narrow finger geometry and high compliance settings on excessive stiffness and limited motion. A wider finger profile (20 mm) was evaluated in G2 (Figure 1b), even though this geometry was previously reported to reduce accessibility in fruit clusters by Williams et al. [2019]. This change isolated the effect of finger width while keeping the same CC and VF = 0.4. G2 satisfied displacement and stress conditions in FEA but contained excessive material due to the high-volume fraction (VF = 0.4, Figure 3b), demonstrating that finger widening alone did not address material efficiency.

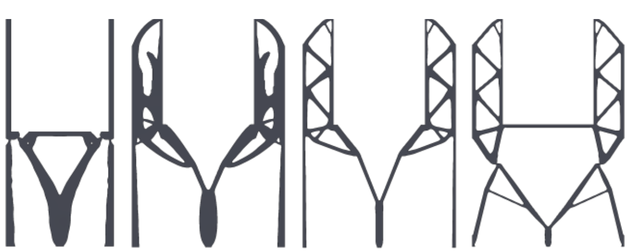

a) b) c) d)

Figure 3: Resulting 3D model. a) G1, b) G2, c) G3, d) G4.

Reducing VF from 0.4 to 0.2 in G3 improved flexibility and allowed full closure motion while maintaining acceptable displacement and stress conditions (Figure 3c). This parameter change confirmed that VF = 0.2 provided sufficient compliance without excessive material use. Finally, G4 reoriented the input point upward instead of downward (Figure 1b). This modification produced an internal beam connecting the two fingers (Figure 3d), increasing local stiffness and causing stress levels to exceed the material limit. Moreover, an experiment involving the removal of this beam demonstrated that a downward input produced the closing motion, while an upward input introduced the opening effect.

4.2 Validation and Material Effects (G5–G6)

The next designs, G5 and G6, were based on an existing rigid gripper layout from Williams *et al.* [2019] (Figure 1c). In G5, placing the input at the right-top corner with minimal fixed support left insufficient room for actuator integration (Figure 4a). This design examined how actuator placement affected finger stability while still meeting simulation constraints. To study stiffness effects, G6 used a shortened version of the same layout (Figure 1d), reducing palm length while keeping VF = 0.2. The smaller design space increased stiffness and therefore raised stress levels for a given displacement. To counter this, the CC was relaxed to 10 N·mm. FEA confirmed these trends: G6 produced slightly lower output displacement and higher stress than G5 but still met preliminary design requirements used in the early stages of this study.

a) b)

Figure 4: Resulting 3D model. a) G5, b) G6.

Despite these limitations, G6 was fabricated and tested using DIC to directly compare experimental displacement–force behaviour with FEA predictions (Figure 5b). Three tests were performed under a 500 g (4.91 N) load, recording displacements until mechanical equilibrium was reached.

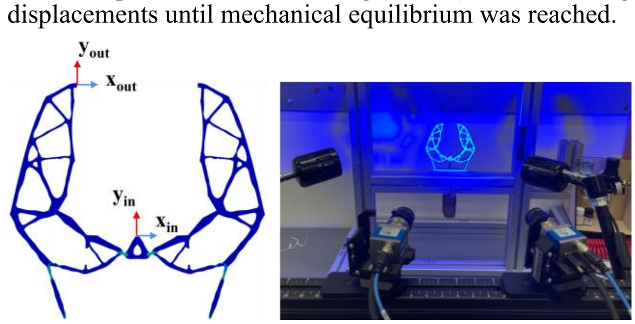

a) b)

Figure 5: FEA and DIC setup for G6. a) FEA, b) DIC

Table 2 shows that DIC consistently recorded larger output displacements than FEA under the same nominal input, with discrepancies in the x- and y-directions reaching nearly twice the predicted values. When the actual DIC-measured displacements were used as FEA boundary conditions, the differences reduced to within 15%, indicating that boundary assumptions, rather than the FEA model itself, caused the initial errors. Importantly, all simulated stresses were far below the manufacturer-reported tensile yield strength of 51 MPa, confirming structural safety even under the largest observed displacements.

The observed differences were primarily attributed to the hygroscopic nature of Nylon White (nylon 6) used in fused filament fabrication [Jia *et al.*, 2004]. Moisture absorption, combined with porosity from layer-by-layer printing [Naresh *et al.*, 2024], likely reduced stiffness and contributed to the larger experimental displacements. Consequently, while nylon was suitable for rapid prototyping, it proved unreliable for high-load or long-term applications.

Table 2: Compares FEA and DIC results for G6

Method	dy_in (mm)	dx_out (mm)	dy_out (mm)	Stress (MPa)
DIC1	-3.79	6.91	-1.58	–
FEA1	-3.79	8.18	-1.87	37.53
DIC2	-4.31	7.88	-1.75	–
FEA2	-4.31	9.31	-2.18	42.74
DIC3	-3.78	6.81	-1.54	–
FEA3	-3.78	8.16	-1.86	37.43
FEA (input = -4.91 N)	-1.95	4.19	-0.87	–

DIC displacements were consistently larger than FEA predictions, with differences up to ~15%, but all stresses remained below the material tensile stress at yield (51 MPa).

Overall, G6 highlighted two critical insights: (i) reducing gripper length increased stiffness, which raised stress concentration and lowered output displacement, and (ii) material selection strongly affects mechanical reliability. These findings informed subsequent designs (G7–G8), emphasizing the need for moisture-insensitive materials, optimized geometry, and careful parameter tuning to balance flexibility, stiffness, and structural performance under harvesting conditions.

4.3 Geometry Refinement and Load Testing (G7)

Building on the parameter insights gained from G1–G6, the G7 prototype (Figure 6) incorporated what appeared to be the optimal configuration: a VF of 0.2 for material efficiency, downward input direction for reliable closure motion. The finger width was increased to 4 mm, providing more material distribution along the fingers and improving stability. Additional non-design regions were introduced to preserve finger geometry and allow future integration of protective sleeves (Figure 1e). FEA confirmed that this configuration achieved the desired displacement and stress performance, satisfying all preliminary design criteria. However, physical testing against the gripping forces reported by Ting [2018] revealed a critical shortcoming: at an applied force of over 50 N, the fingers bent outward, and the gripper failed to securely retain the kiwifruit during closure, leading to fruit slippage.

This outcome highlighted two key limitations. First, the finger width should gradually increase from the tip to the base to maintain stiffness during gripping while still allowing access to fruit clusters. Second, locating the output at the fingertip provided higher displacement but at the cost of reduced stiffness and less effective force transmission. These findings confirmed that even with parameter optimization, geometric stiffness and load-distribution characteristics required further refinement for harvesting applications.

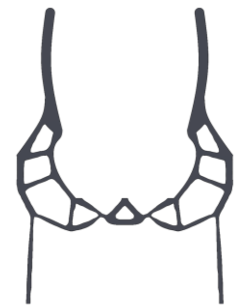

Figure 6: Resulting 3D model of G7.

4.4 Synthesis of Insights from G1–G7

Table 3 summarises the results across all prototypes (G1–G7) and illustrates the iterative learning process that informed the final design. Several trends emerged:

- *Finger geometry and width:* Narrow fingers in G1 produced excessive stiffness and deformation due to high CC, while wider fingers in G2 and G3 improved displacement but reduced accessibility in fruit clusters. The introduction of non-design regions in G7 preserved finger shape while enabling sleeve integration and force transmission.
- *Material distribution:* High VF (0.4) in G1–G2 produced unnecessary stiffness and material waste, whereas VF = 0.2 (G3–G7) achieved sufficient flexibility for closure while limiting material usage. Low CC values concentrated material less at the flexure hinges, making the mechanism more compliant and lowering input force requirements but also increasing local stress. In contrast, higher CC values distributed material more evenly, reducing stress concentration but limiting displacement and requiring higher input forces.
- *Input direction and output position:* Upward input in G4 produced undesirable loading and internal beam formation, while downward input consistently produced reliable closure motion across all subsequent designs. Relocating the output from the fingertip to the middle of the finger is necessary to balance stiffness and flexibility.
- *Material and environmental effects:* DIC–FEA comparisons in G6 revealed that nylon prototypes exhibited moisture-induced softening, leading to an increase in displacement under load. This emphasized the need for material selection to complement geometric optimization.

Taken together, these findings defined the requirements for the final design: downward input for closure reliability, middle of the finger output for balanced displacement and stiffness, new finger shape to prevent bending, non-design regions for geometry control and sleeve integration. These requirements directly informed the development of the final prototype, G8.

Table 3: Performance summary for prototypes G1–G7, highlighting displacement behaviour, stress margins relative to yield strength, and qualitative insights guiding parameter refinement toward the final design (G8).

Model	Max Displacement	Stress and Yield	Performance and Insights
G1	Low (fragile design)	Exceeded limit	Too stiff; narrow finger; high CC limits motion
G2	Moderate	Within limit	Wide finger improves stiffness but reduces efficiency
G3	High (full closure)	Within limit	VF = 0.2 gives better flexibility & closure
G4	Low	Exceeded limit	Upward input creates internal beam; high stresses
G5	Moderate	Within limit	Limited actuator space; rigid reference design
G6	Moderate	Within limit	DIC > FEA by ~15%; moisture-sensitive nylon reduces reliability
G7	High	Within limit	Failed at high loads; finger bends; and insufficient stiffness

Preliminary physical gripping force was only evaluated for G7 since earlier designs failed functional criteria (finger shape).

4.5 Final Design (G8)

The final design, G8 (Figure 7), was developed using DS6 (Figure 1f) and incorporates all insights gained from prototypes G1–G7, with the exception of moisture sensitivity, which remains an area for future investigation. Subsequent studies will examine alternative 3D printing methods (e.g., Selective Laser Sintering (SLS) with polyamide 12 (PA12, nylon 12) powder, which offers a strength-to-stiffness ratio similar to that of the current material) as well as other moisture-resistant materials to mitigate environmental effects on structural performance.

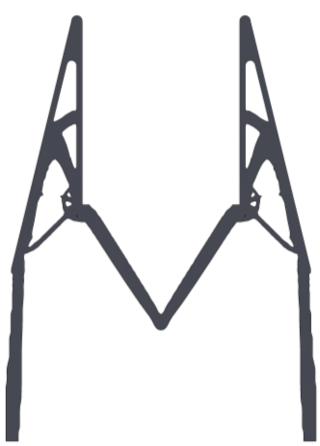

Figure 7: Resulting 3D model of G8.

The G8 configuration was specifically designed to meet the 50 N gripping force requirement identified in kiwifruit harvesting studies [Ting, 2018]. Finite element analysis (FEA) first confirmed that the final design satisfied all key performance criteria: displacement, stress limits, and gripping force, while remaining safely below the material yield strength (Figure 8). Building on these findings, initial testing of the 3D-printed prototype demonstrated that the bending and stiffness limitations observed in G7 were successfully resolved in G8, validating the geometric and structural refinements introduced during the iterative process. Quantitatively, the simulation results showed that an input force of 190 N produced a displacement of 7.79 mm at the middle of the finger, corresponding to an estimated gripping force of 54 N, which satisfied the required threshold for secure fruit retention under operational conditions. Experimental validation is now underway to confirm these simulation predictions through controlled laboratory testing, followed by field trials under realistic harvesting environments to assess long-term performance and durability.

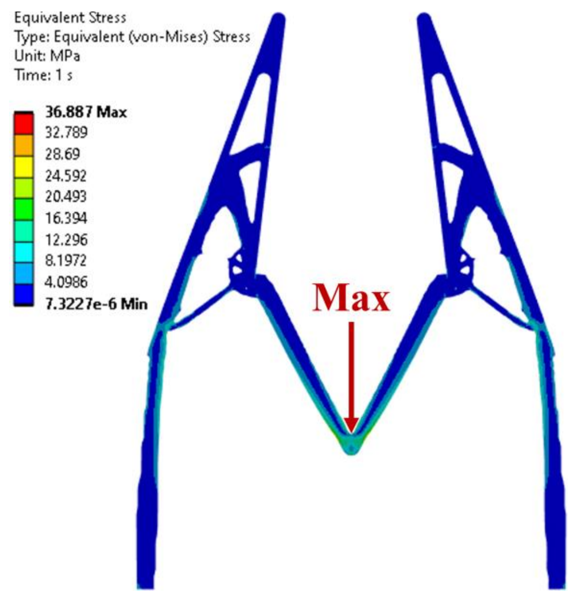

Figure 8: FEA of the G8 gripper stress distribution at a grasping distance corresponding to a minimum-sized kiwifruit.

Overall, by integrating parameter and geometric refinement, G8 represents the final outcome of the iterative design process. It provides the first prototype to simultaneously satisfy flexibility, stiffness, load capacity, and harvesting functionality requirements. The current gripper is designed for orchard conditions with dense fruit clusters and operates across the commercial size range of green and gold kiwifruit. The scalability of the gripper is considered based on the characteristics of each fruit species and the requirements of other systems.

Future work will focus on extended field-based validation, evaluation of alternative materials beyond nylon, and fatigue-life assessment under repeated loading cycles to establish the long-term suitability of G8 for robotic kiwifruit harvesting applications.

5 Conclusion

This study presented a parameter-driven design exploration for developing a two-finger compliant gripper for kiwifruit harvesting using 2D topology optimization. Through eight successive prototypes, systematic variation of design space, boundary conditions, and optimization parameters established clear relationships between design choices and functional performance. Among the key findings, mid-span output placement achieved the best balance between displacement capacity and structural stiffness, while downward actuation consistently produced more reliable closing motion than upward input. A VF of 0.2 maintained adequate flexibility without unnecessary material use, and careful tuning of the CC improved stress distribution while preserving structural integrity. The final prototype (G8) successfully met all displacement, stress, gripping force, and functional requirements, demonstrating the potential of compliant grippers developed through structured parameter exploration. Initial comparisons between simulation and experimental results, particularly for moisture-sensitive nylon prototypes, underscore the importance of investigating alternative materials to ensure reliable field performance. Ongoing experimental testing will validate the G8 design under laboratory and orchard conditions, while future work will extend this approach toward a standardized design workflow integrating alternative materials, advanced additive manufacturing methods, and comprehensive field trials for robotic kiwifruit harvesting applications. Furthermore, pneumatic actuation will be used to enhance responsiveness and simplify control. Efficiency will be monitored and energy consumption reduced through leakage reduction, flow control, and timing optimization, while preserving grip performance.

Acknowledgements

This research was funded by the Ministry of Business, Innovation and Employment (MBIE), New Zealand, under grant UOWX2203. The project is a collaboration between the University of Waikato and the University of Auckland. We thank the technical staff at the School of Engineering, University of Waikato, for their support during the work. We also thank Dr. Dorota Budzyń for her help in explaining how to use the Topology Optimization method in Altair OptiStruct (HyperWorks). The authors also used the language editing tool GPT-5 to improve readability. The authors reviewed and edited the content and take full responsibility for the publication.

References

[Budzyń, 2024] Dorota Budzyń. Compliant mechanisms in lunar surface exploration: design and technology considerations for dust mitigation. PhD thesis, *University of Glasgow*.

[Budzyń, 2023] Dorota Budzyń, Hossein Zare-Behtash, Aidan Cowley, and Andrea Cammarano. Implicit Lunar Dust Mitigation Technology: Compliant Mechanisms. *Acta Astronautica*, 203(146--156), 2023.

[Fu, 2024] Min Fu, Shike Guo, Anyu Chen, Renxuan Cheng, and Xiaoman Cui. Design and experimentation of multi-fruit envelope-cutting kiwifruit picking robot. *Frontiers in Plant Science*, 15(1338050), 2024.

[Gallego and Herder, 2009] Juan A. Gallego and Just Herder. Synthesis Methods in Compliant Mechanisms: An Overview. In *Proceedings of the ASME 2009 International Design Engineering Technical Conferences and Computers and Information in Engineering Conference*, pages 193--214, City, 2009.

[Howell, 2001] Larry L. Howell. *Compliant Mechanisms*. Wiley, 2001.

[Jia, 2004] Nanying Jia, Howard A Fraenkel, and Val A Kagan. Effects of moisture conditioning methods on mechanical properties of injection molded nylon 6. *Journal of reinforced plastics and composites*, 23(7): 729--737, 2004.

[Liu, 2018] Chih-Hsing Liu, Ta-Lun Chen, Chen-Hua Chiu, Mao-Cheng Hsu, Yang Chen, Tzu-Yang Pai, Wei-Geng Peng, and Yen-Pin Chiang. Optimal Design of a Soft Robotic Gripper for Grasping Unknown Objects. *Soft Robotics*, 5(4): 452-465, 2018.

[Liu, 2024] Chih-Hsing Liu, Yi-Chieh Shih, and Jui-Chih Chi. Topology Optimization and Prototype of a Highly Adaptive Multi-Material Compliant Finger for Parallel Grippers. *IEEE Robotics and Automation Letters*, 2024.

[Miao and Zheng, 2020] Yubin Miao and Jiafeng Zheng. Optimization Design of Compliant Constant-force Mechanism for Apple Picking Actuator. *Computers and Electronics in Agriculture*, 170(105232), 2020.

[Mu, 2020] Longtao Mu, Gongpei Cui, Yadong Liu, Yongjie Cui, Longsheng Fu, and Yoshinori Gejima. Design and simulation of an integrated end-effector for picking kiwifruit by robot. *Information Processing in Agriculture*, 7(1): 58--71, 2020.

[Naresh, 2024] Dharavathu Naresh, Ramesh Raju, and Shekera Parveen. Design and development of alternate layer printing method to reduce the porosity in FDM printing process. *International Journal on Interactive Design and Manufacturing (IJIDeM)*, 18(5): 3439--3448, 2024.

[Rajendran, 2024] Vishnu Rajendran, Bappaditya Debnath, Sariah Mghames, Willow Mandil, Soran Parsa, Simon Parsons, and Amir Ghalamzan-E. Towards autonomous selective harvesting: A review of robot perception, robot design, motion planning and control. *Journal of Field Robotics*, 41(7): 2247--2279, 2024.

[Saeed, 2021] Munazza Saeed. Labour Shortage–The Role of Technology Led Innovation in the Kiwifruit Industry. *KELLOGG Rural Leadership Programme*. Retrieved 22 June 2024 from https://ruralleaders.co.nz/wp-content/uploads/2021/11/Munazza-Saeed-The-role-ot-technology-led-innovation-in-the-Kiwifruit-Industry-K44-2021.pdf

[Sun, 2022] Yilun Sun, Yuqing Liu, Felix Pancheri, and Tim C Lueth. Larg: A Lightweight Robotic Gripper with 3-d Topology Optimized Adaptive Fingers. *IEEE/ASME Transactions on Mechatronics*, 27(4): 2026--2034, 2022.

[Ting, 2018] Chia-nan Ting. Comparison Between Selective and Non-selective Kiwifruit Harvesters for Economic Viability. Master thesis, *The University of Waikato*.

[Wang, 2020] Rixin Wang, Xianmin Zhang, Benliang Zhu, Hongchuan Zhang, Bicheng Chen, and Haonan Wang. Topology Optimization of a Cable-Driven Soft Robotic Gripper. *Structural and Multidisciplinary Optimization*, 62(2749--2763), 2020.

[Williams, 2019] Henry Williams, Canaan Ting, Mahla Nejati, Mark Hedley Jones, Nicky Penhall, JongYoon Lim, Matthew Seabright, Jamie Bell, Ho Seok Ahn, Alistair Scarfe, Mike Duke, and Bruce MacDonald. Improvements to and large-scale evaluation of a robotic kiwifruit harvester. *Journal of Field Robotics*, 37(2): 187--201, 2019.

[Xiao, 2024] Xu Xiao, Yaonan Wang, and Yiming Jiang. Review of research advances in fruit and vegetable harvesting robots. *Journal of Electrical Engineering & Technology*, 19(1): 773--789, 2024.

[Xie, 2022] Huaibei Xie, Deyi Kong, and Qiong Wang. Optimization and experimental study of bionic compliant end-effector for robotic cherry tomato harvesting. *Journal of Bionic Engineering*, 19(5): 1314--1333, 2022.

[Zhiwei, 2025] Tian Zhiwei, Guo Xiangyu, Ma Wei, and Xue Xinyu. Research on kiwifruit harvesting robot worldwide: A solution for sustainable development of kiwifruit industry. *Smart Agricultural Technology*, 100792, 2025.

[Zolfagharian, 2022] Ali Zolfagharian, Saleh Gharaie, Jack Gregory, Mahdi Bodaghi, Akif Kaynak, and Saeid Nahavandi. A Bioinspired Compliant 3D-printed Soft Gripper. *Soft Robotics*, 9(4): 680--689, 2022.